On the role of free carboxylic groups and cluster conformation on the surface scratch healing behaviour of ionomers

J.M. Vega [a,b], A.M. Grande [a], S. van der Zwaag [a], S.J. Garcia [a,*]

[a] Novel Aerospace Materials Group, Faculty of Aerospace Engineering, Delft University of Technology, Kluyverweg 1, 2629 HS Delft, The Netherlands
[b] Materials Innovation Institute, Mekelweg 2, 2600 GA Delft, The Netherlands

Article history:
Received 1 March 2014
Received in revised form 29 April 2014
Accepted 8 May 2014
Available online 20 May 2014

1. Introduction

Intrinsic healing polymers are materials in which the healing capability is provided by the polymer network itself which increases its mobility upon a certain minimal chemical, mechanical or thermal energy input. In the case of healing polymers using reversible chemistries the increased mobility leads to a local viscous flow of the material in the vicinity of the damage site followed by a process of spontaneous restoration of the chemical and physical bonds and a (partial) recovery of the original mechanical or functional properties [1]. One of the first and most studied intrinsic self-healing polymers are the so-called ionomers as these have shown the ability to autonomously close and seal holes produced by pointed high speed impact objects [2–4]. Ionomers are partially neutralized polymers which bulk properties are deeply affected by ionic interactions within discrete regions of the polymer structure [5]. The strong Coulombic interactions between the ion pairs yields ionic aggregates acting as multifunctional "electrostatic" crosslinks [6] and as a result, a supramolecular network (spatially distributed clusters) of physical (reversible) crosslinks are formed. The final polymer structure and thus physical and mechanical properties strictly depend on neutralization level and neutralizing ions [7,8]. Likewise it is also expected that the polymer architecture will have a major influence on the healing capabilities of intrinsic healing polymers [9].

Ionomers are currently being considered for relatively new applications [10]. In particular their adequate mechanical properties in combination with a remarkable autonomous healing capability after ballistic impact at low, mid and hyper velocities [11] have led to various suggested applications such as multilayer composites for spacecraft debris protection shields [12] and self-sealing layers in tank reservoirs for low velocity impact [4,13]. In order to further extend their application range without losing their most crucial properties ionomers have been blended with other polymers this leading to significant improvements [14,15].

* Corresponding author. Tel.: +31 (0)152781637; fax: +31 (0)152784472.
E-mail address: s.j.garciaespallargas@tudelft.nl (S.J. Garcia).

Upon ballistic impact there is substantial but undefined degree of heating of the region close to the impact site due to the work of bullet-polymer friction and the work of deformation. As a result, the material is raised to a temperature well above both the declustering and secondary crystal phase melting temperature (or characteristic ionomer transition temperatures) [16,17] and even above the primary crystal phase melting temperature. The actual healing after passage of the bullet proceeds via a two stage-process with a fast initial elastic recovery of the molten material, followed by a much slower viscoelastic response leading to inter-diffusion and reformation of the original ionomer microstructure [4,18]. Most studies on the healing mechanism of ionomers found in literature focused on elucidating the role of the neutralization level and the cluster content in the healing process after ballistic impact [18–20] with almost no focus on the possible effect of amount of free carboxylic groups identified by Kalista as a potential driver for the healing process [4]. In more recent times the effect of phase morphology on the healing efficiency in ionomers and ionomer based blends has gained attention [18,21]. Puncture studies performed under pseudo-static conditions highlighted the importance of the microstructure controlling the elastic response involved in the healing process [22]. Despite all these efforts, and while it is clear the relevance of polymer architecture on healing [9], the role of the different physical and chemical parameters in the healing of ionomers is not yet clear. The lack of clarity is the unavoidable result of the highly transient and poorly defined state of the ballistic impact site with large gradients in both the local deformation and the thermal fields.

In this work we introduce the use of well controlled scratching experiments at room temperature with subsequent isothermal healing treatments to separate in a more controlled way the viscoelastic and viscoplastic contributions to healing. The role of clusters and carboxylic groups in the healing process of poly[ethylene-co-(methacrylic acid)] ionomers at temperatures well below the polymer melting temperature was elucidated. The equilibrium cluster state as well as the number of free carboxylic end groups was varied intentionally by blending the ionomer with adipic acid, which is known to have a large effect on the ballistic healing behaviour [18,22]. The surface scratch healing behaviour is analysed by confocal microscopy and linked to the chemical and microstructural information obtained from additional infrared and X-ray tests.

2. Experimental section

2.1. Materials

In this study two series of poly(ethylene-co-methacrylic acid) zinc ionomer based blends (Table 1) were prepared using a mini-extruder with a twin screw configuration at 150 °C with the aim of varying the free carboxylic content as well as the equilibrium cluster content:

- Series 1 (EMAA-Zn/EMAA): Pellets of Nucrel 960® (DuPont™) containing 5.4 mol% of methacrylic acid groups (MAA) were blended in different proportions with pellets of Surlyn 9520® (Dupont™) containing 3.5 mol% MAA out of which 71% were neutralized with Zn^{2+} ions.
- Series 2 (EMAA-Zn/AA): Pellets of Surlyn 9520® (EMAA-Zn) were blended in different proportions with adipic acid powder (AA), $(CH_2)_4(COOH)_2$.

After blending and palletising the extrudate two types of specimens were prepared by compression moulding using a hot press: (i) ionomer coated galvanized steel plates for scratch healing tests and (ii) free standing ionomer films for general polymer characterization. The compression moulding was performed at a pressure of 0.67 MPa, a mould temperature of 130 °C and a pressing time of 5 min. Kapton® foils were used to separate the samples from the heated flat die surfaces. The samples were water-cooled to room temperature before releasing the pressure. The thickness of both coatings and free-standing films was around 160 ± 10 μm as measured by a PosiTector® 6000 thickness gage. The coatings and films had a smooth surface and a homogeneous appearance. After moulding the samples were stored at room temperature for at least 30 days to equilibrate the microstucture. The equilibration conditions were based on earlier work on the kinetics of the secondary phase formation [23].

2.2. Scratch procedure and healing quantification

For the creation of well-controlled surface scratches a microscratch tester (MST) from CSM Instruments with a 100 μm radius sphere-conical diamond indenter tip (Rockwell) was used. The scratch length (5 mm), load (2 N) and the scratching speed (10 mm/min) were kept constant in all experiments. Four scratches were created per sample.

The scratching procedure consisted of the following steps:

(i) A pre-scan at 0.03 N load. This step allows automatic correction during the scratch process for sample tilting or topology variations.
(ii) A scan at a 2 N load. This scan creates a surface deformation of the polymer (scratch) with a maximum penetration depth (P_d) as shown in Fig. 1a.
(iii) A post-scan at 0.03 N load. This step allows determination of the scratch depth just after load (R_d) and determination of the fast viscoelastic recovery. The residual depth (R_d) is also indicated schematically in Fig. 1a.

The immediate viscoelastic recovery (VE_R) was quantified using the parameters directly given by the MST instrument during the scratch procedure (P_d and R_d) using the following equation [24]:

$$VE_R(\%) = (1 - R_d/P_d)100 \quad (1)$$

The change in scratch profile and depth (at room temperature) after stepwise annealing at a fixed temperature of 70 °C for times up to 240 min was measured with a laser scanning confocal microscope Olympus OLS 3100 (software LEXT OLS 6.0.11) using a 20× objective. The

Table 1
Overview of the sample coding and the blend compositions.

EMAA-Zn/EMAA blends			EMAA-Zn/AA blends		
Sample code	EMAA-Zn (wt.%)	EMAA (wt.%)	Sample code	EMAA-Zn (wt.%)	AA (wt.%)
100/0	100	0	100/0	100	0
53/47	53	47	99/1	99	1
30/70	30	70	97/3	97	3
10/90	10	90	94/6	94	6
0/100	0	100	90/10	90	10
			80/20	80	20

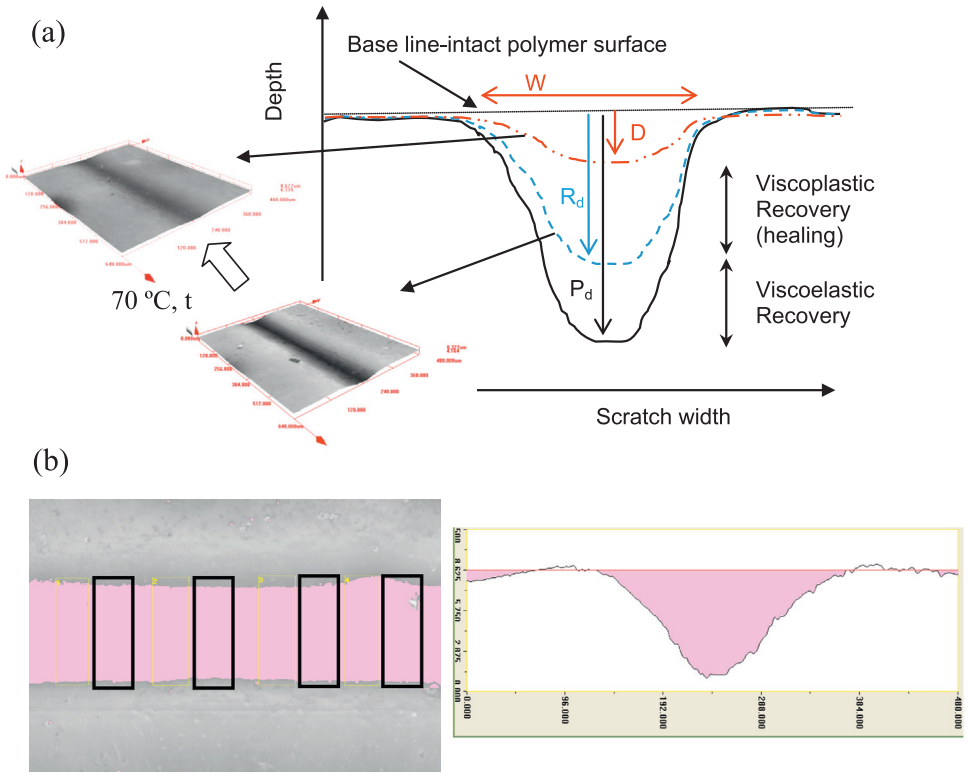

Fig. 1. (a) Evolution of a scratch profile showing the initial viscoelastic recovery and the temperature triggered viscoplastic recovery (healing). Inserts are confocal images of a damaged and healed scratch. (b) Surface area (left) and scratch profile (right) after threshold selection for the quantification of healing efficiency as seen in Eq. (2). The black rectangles indicate the four zones used to measure the cross sectional profile. All results to be presented in this work were obtained after 30 min sample exposure to 70 °C.

samples were taken out of the oven every 30 min and allowed to equilibrate at room temperature for additional 30 min before evaluation with the confocal microscope. A healing temperature of 70 °C was selected as it is above the multiple transition temperatures (35–55 °C) but below the primary melting temperature (93–97 °C) of the materials studied.

Our preliminary work on scratch healing kinetics of polymers has shown that the most appropriate parameter to quantify healing efficiency with low experimental error is the determination of the cross sectional area of the scratch below the original sample surface level. Fig. 1b shows the surface and profile of a scratch after threshold selection. The scratch healing efficiency was quantified using the following equation:

$$\textit{Healing Efficiency}(\%) = 100 - \left(\frac{(V/A)_{A.H.}}{(V/A)_{B.H.}}\right)100 \qquad (2)$$

where *V/A* is the volume/area ratio after healing (*A.H.*) and before healing (*B.H.*).

The average scratch volume was determined by measuring four cross sectional areas at different locations in the central part of the scratch. This work focuses on the processes related to the thermally activated viscoplastic recovery (healing) as described in Eq. (2).

2.3. Fourier transform infrared spectroscopy

Fourier transform infrared spectroscopy (FTIR) was performed using a Perkin–Elmer Spectrum 100 FTIR. The

spectra for a particular polymer and condition were obtained using 8 scans across a range of 4000–550 cm^{-1}. All IR spectra were normalized using the peak at 2916 cm^{-1} related to the C—C bond. The content of free carboxylic groups can be obtained from the normalized FTIR spectra by calculating the area of the peak at 1257 cm^{-1} divided by the area of the peak at 2916 cm^{-1}.

2.4. X-ray diffraction

A Brueker D8 Discover X-ray diffractometer equipped with a 2-dimensional Hi-Star Area Detector and Cross Coupled Göbel Mirrors was used to determine the diffractogram of the polymer systems prior to scratching and healing. The measurements were performed in transmission mode at room temperature using monochromatic Cu Kα radiation and a sample to detector distance of 30 cm. The relative cluster content was determined by integration of the wide-angle X-ray scattering (WAXS) profile over $3° < 2\theta < 10°$. The selection of this range for the quantification of the cluster content has established in agreement with previous works where the thicker amorphous region observed at low 2θ was attributed to the presence of ionic aggregates or clusters [7,16,25,26].

3. Results

3.1. Cluster content

Fig. 2 shows the WAXS spectra of both series of blends (EMAA-Zn/EMAA and EMAA-Zn/AA). Both series show a clear decrease in the cluster content upon blending EMAA or AA into the EMAA-Zn ionomer as shown by the decrease in the XRD signal at low 2θ. The crystalline peaks related to the polyethylene crystals in the EMAA-Zn are slightly altered due to blending this suggesting a slight effect also on the primary crystal phase.

3.2. Free carboxylic content

Fig. 3a shows the evolution of the FTIR spectra for the EMAA-Zn/EMAA blends. The asymmetric methyl deformation peak at 1464 cm^{-1}, the methyl rocking peak at 719 cm^{-1}, and the peaks at 1407 and 1381 cm^{-1} [27,28] do not seem to undergo significant changes with the blending process or the neutralization level. This is taken to be an indication that the main polymer backbone is not altered significantly due to the neutralization or the blending process. From the broad out-of-plane O–H bending peak at ~938 cm^{-1} it is clear that carboxylic acid groups exist predominantly as dimers in the polymer backbone [29]. The number of dimers (considered here on as "free" carboxylic groups) is strongly reduced in the Zn ionomer with respect to the EMAA sample (the peak becomes almost negligible at 938 cm^{-1}) but the signal increases again in the EMAA-Zn/EMAA blends, clearly indicating an increase of the free carboxylic groups content upon blending. A similar result was obtained for the EMAA-Zn/AA blends.

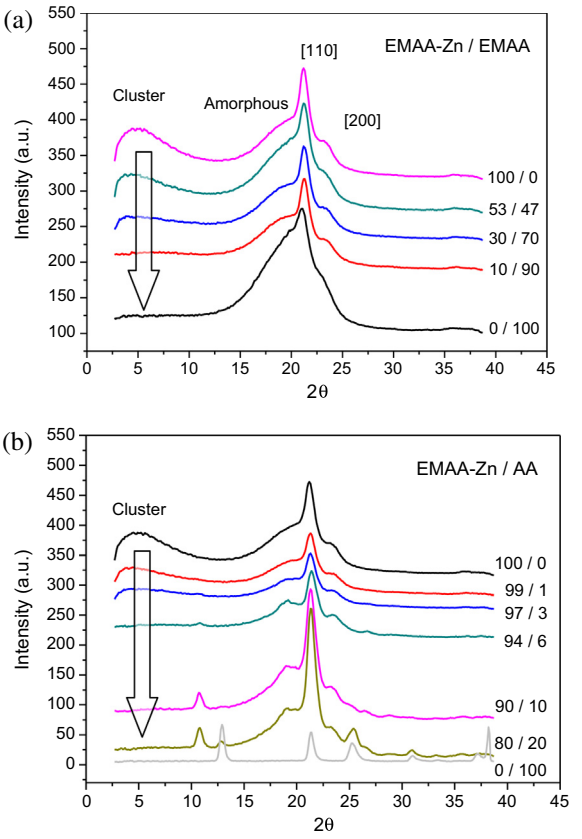

Fig. 2. X-ray spectra of the EMAA-Zn/EMAA (a) and EMAA-Zn/AA (b) blends. Arrow indicates decrease in cluster content.

Fig. 3b shows a plot of the free carboxylic groups calculated in two manners: (i) as the theoretical content of free COOH groups calculated from the carboxylic content of the base polymers and blend ratios and (ii) the free carboxylic groups content determined by FTIR. The plot shows good agreement between the two methods for both series of blends. This validates the use of FTIR for the calculation of free carboxylic groups in the present study.

4. Discussion

Fig. 4 shows the effect of the free carboxylic groups content and cluster fraction on the scratch healing efficiency respectively. In particular, observing Fig. 4a it is evident that the increase of free carboxylic groups with either of the two blending approaches (blending with EMAA or with adipic acid) leads to a clear increase of the healing efficiency up to a maximum of around 65–70%. The data for the EMAA/EMAA-Zn blends and the EMMA-ZN/AA blends are described by a single master curve.

The presence of ionic aggregates affects not only the microstructure but also produces a decrease in polymer crystallinity and in the amorphous phase mobility [30]. These aspects could have a direct effect on the healing behaviour as both parameters reduce the ability to recover large local viscoplastic deformations as induced in

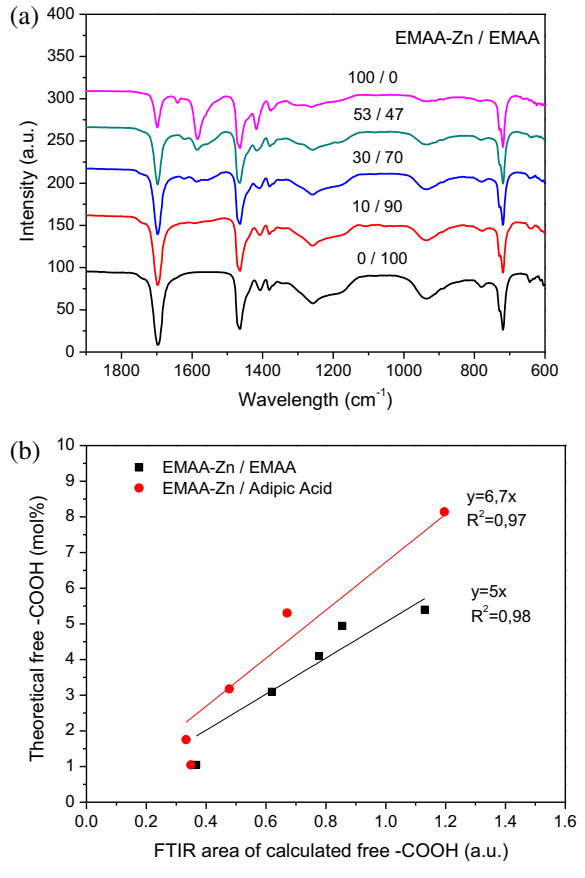

Fig. 3. Evolution of the FTIR spectra in EMAA-Zn/EMAA blends (a) and correlation between the calculated free COOH content and the FTIR peak area for EMAA-Zn/EMAA and EMAA-Zn/AA (b).

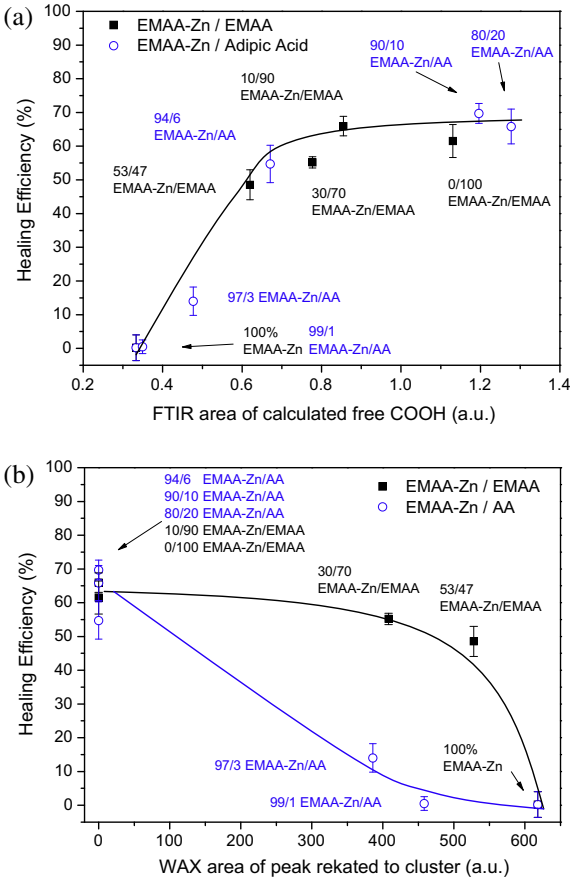

Fig. 4. Effect of the free carboxylic content (a) and cluster content (b) on the healing efficiency of EMAA-Zn/EMAA (■) and EMAA-Zn/AA (○) blends. Cluster and COOH content increase to the right.

scratching experiments. On the other hand, the free COOH content is known to diminish the formation of crystalline phase, thus promoting a positive effect on the recovery performances [31]. It is clear that the balance between the crystal content and the amorphous phase properties, both affected by the ionic aggregate state and the free COOH content, plays a crucial role in the healing behaviour.

From these results it is apparent that the maximum healing efficiency was already obtained at an FTIR area of calculated free COOH of 0.7–0.75 (a.u.) which corresponds to 3–3.5% content of free carboxylic groups as extrapolated from Fig. 3b 3–3.5% of free carboxylic groups is hence the minimum necessary amount to reach the maximum healing efficiency, while values above this do not bring any significant increase in the healing efficiency, irrespective of the blend series.

Furthermore, analysing the healing efficiency as a function of the cluster content (Fig. 4b), a clear dependency on the type of blend is observed. While EMAA-Zn/EMAA blends show a fast increase of the degree of healing by slightly decreasing the cluster content, the EMAA-Zn/AA blends show a significant increase in healing only when clusters have practically disappeared.

The trends observed in Fig. 4a and b show a clear dependency of the healing efficiency with the free carboxylic groups and cluster content and highlight the effect of the different blends employed in this study. Blending EMAA-Zn with EMAA leads to an increase of COOH and a decrease in cluster content. On the other hand, blending EMAA-Zn with adipic acid leads to cluster destruction and increase of healing efficiency. In this case, small amounts of adipic acid (6%) lead to the total disappearance of clusters. When comparing Fig. 4a and b, it becomes clear that a high healing efficiency can be obtained with 3% of free COOH groups even when a significant amount of cluster content is present. The disappearance of clusters does not lead to a significant change of surface scratch healing efficiency, highlighting the dominance of free COOH content over the cluster content in the low temperature healing efficiency.

Additional experiments were designed to demonstrate the presumed correlation between polymer microstructure and healing efficiency. For this test, samples from the EMAA-Zn/EMAA blend series were annealed for 3 h at 70 °C to make sure that the secondary crystal phase was dissolved [32,33]. Then the samples were cooled to room temperature and the samples were scratched and

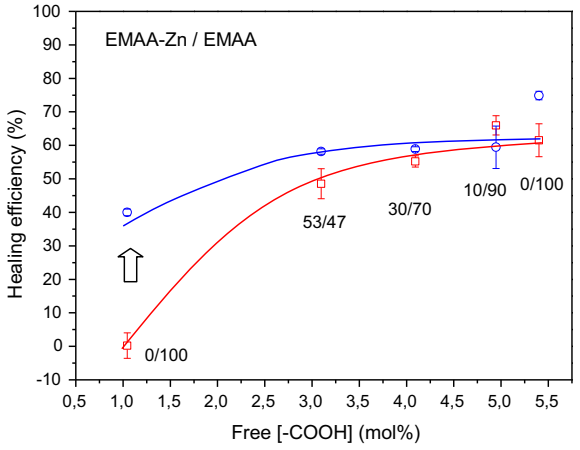

Fig. 5. Effect of annealing in the healing efficiency of an EMAA-Zn/EMAA blend. Red squares are non-annealed samples (□), blue circles are annealed (○). (For interpretation of the references to colour in this figure legend, the reader is referred to the web version of this article.)

measured within 30 min after the annealing. The results of this test are shown in Fig. 5. For samples with a high free carboxylic content the prior dissolution of the crystal organization in the amorphous phase did not lead to a significant change in healing efficiency. For the samples with a low free carboxylic content (i.e. having a higher secondary crystal phase content) the prior dissolution of the clusters led to a significant increase in the healing efficiency, although to a value below that of samples with a high free carboxylic content. Also in this case a COOH content above 3% was shown to lead to optimal healing and the presence of clusters played a marginal role in the healing process. This finding is in good agreement with previous studies where the healing of ionomers was linked to their viscoelastic response after ballistic impact [19]. In this study the fine control of the damage and healing quantification achieved by means of surface scratch experiments significantly adds to the understanding of the key factors leading to healing in ionomers further establishing the minimum free COOH content required for the maximum healing response.

5. Conclusions

The study revealed that both the cluster and the free carboxylic groups content have an influence on the viscoplastic response and hence on the healing efficiency. It is found that 3% of free carboxylic groups leads to the maximum scratch healing efficiency possible (65%) independently of the cluster state. The results found in this work suggest that the carboxylic group content may be a more important parameter in the healing process than the cluster content.

Acknowledgements

This research was carried out under projects M41.6.10400 and M41.6.12456 in the framework of the Research Program of the Materials innovation institute M2i (www.m2i.nl). The authors want to acknowledge N.V. Bekaert S.A. and DuPont™ for material supply and Mr. Christian Mathis for his help in defining procedures to quantify surface scratch healing. Mr. Ben Norder is acknowledged for the assistance with the WAXS measurements.

References

[1] Garcia SJ, Fischer HR, van der Zwaag S. Prog Org Coat 2011;72:142–9.
[2] Seibert GM. US Patent 5.486.425; 1996.
[3] Fall R. Puncture reversal of ethylene ionomers-mechanistic studies. Master of Science. Blacksburg: Virginia Polytechnic Institute and State University; 2001.
[4] Kalista SJ, Ward TC, Oyetunji Z. Mech Adv Mater Struct 2007;14:391–7.
[5] Eisenberg A, Rinaudo M. Polym Bull 1990;24. 671-671.
[6] Eisenberg A, Hird B, Moore RB. Macromolecules 1990;23:4098–107.
[7] Tadano K, Hirasawa E, Yamamoto H, Yano S. Macromolecules 1989;22:226–33.
[8] Han K, Williams HL. J Appl Polym Sci 1991;42:1845–59.
[9] Garcia SJ. Eur Polym J 2014;53:118–25.
[10] Zhang L, Brostowitz NR, Kevin A, Cavicchi KA, Weiss RA. Macromol React Eng 2014;8:81–99.
[11] Grande AM, Castelnovo L, Di Landro L, Giacomuzzo C, Francesconi A, Rahman MA. J Appl Polym Sci 2013;130:1949–58.
[12] Francesconi A, Giacomuzzo C, Grande AM, Mudric T, Zaccariotto M, Etemadi E, et al. Adv Space Res 2013;51:930–40.
[13] Coughlin CS, Martinelli AA, Boswell RF. Abstr Papers Am Chem Soc 2004;228:261.
[14] Rahman MA, Penco M, Peroni I, Ramorino G, Grande AM, Di Landro L. ACS Appl Mater Interfaces 2011;3:4865–74.
[15] Rahman MA, Penco M, Spagnoli G, Grande AM, Di Landro L. Macromol Mater Eng 2011;296:1119–27.
[16] Quiram DJ, Register RA. Macromolecules 1998;3:1432–5.
[17] Loo Y, Wakabayashi K, Huang YE, Register RA, Hsiao BS. Polymer 2005;46:5118–24.
[18] Varley RJ, van der Zwaag S. Acta Mater 2008;56:5737–50.
[19] Varley RJ, Shen S, van der Zwaag S. Polymer 2010;51:679–86.
[20] Kalista SJ, Pflug JR, Varley RJ. Polym Chem 2013;4:4910–26.
[21] Rahman MA, Spagnoli G, Grande AM, Di Landro L. Macromol Mater Eng 2013;298:1350–64.
[22] Varley RJ, van der Zwaag S. Polym Int 2010;59:1031–8.
[23] Spencer MW, Wetzel MD, Troeltzsch C, Paul DR. Polymer 2012;53:569–80.
[24] Brostow W, Bujard B, Cassidy PE, Hagg HE, Montemartini PE. Mater Res Innov 2002;6:7–12.
[25] Kutsumizu S, Tadano K, Matsuda Y, Goto M, Tachino H, Hara H, et al. Macromolecules 2000;33:9044–53.
[26] Taubert A, Winey KI. Macromolecules 2002;35:7419–26.
[27] Painter PC, Watzek M, Koenig JL. Polymer 1977;18:1169–72.
[28] Painter PC, Brozoski BA, Coleman MM. J Polym Sci Part B 1982;20:1069–80.
[29] Siuzdak DA, Start PR, Mauritz KA. J Appl Polym Sci 2000;77:2832–44.
[30] Wakabayashi K, Register RA. Macromolecules 2006;39:1079–86.
[31] Wakabayashi K, Register RA. Polymer 2005;46:8838–45.
[32] Kohzaki M, Tsujita Y, Takizawa A, Kinoshita T. J Appl Polym Sci 1987;33:2393–402.
[33] Kuwabara K, Horii F. J Polym Sci Part B 2002;40:1142–53.